Data-Driven and Physics-Informed Machine Learning for Outdoor Acoustic Wave Modeling using the Linearized Euler Equations

Hessel Juliust[1,2], Katharina Baumann[1], Arthur Schady[1], Sirine Gharbi[1], Felix Dietrich[2]
[1] *Institute of Atmospheric Physics, German Aerospace Center*
[2] *School of Computation, Information and Technology, Technische Universität München*
Corresponding Email: hessel.juliust@dlr.de

Introduction

Modeling of outdoor acoustic wave propagation is crucial for diverse applications, including noise mapping for urban planning [1], environmental monitoring [2], and aviation acoustics [3]. The propagation of acoustic waves outdoors is strongly influenced by atmospheric conditions, such as wind and temperature gradients [2], and interactions with topographic features, making accurate predictions challenging.

The Linearized Euler Equations (LEE) provide a mathematical framework capable of modeling acoustic wave propagation in the atmosphere by capturing the interactions between acoustic velocity, pressure fluctuations, and atmospheric flow fields [4, 5]. However, because of its wave behavior, solving it with traditional numerical methods such as finite-difference time-domain (FDTD) [6, 7] requires substantial computational resources, especially for high-frequency scenarios and large spatial domains [8]. Moreover, these methods typically rely solely on predefined physical assumptions without leveraging available simulation or measurement data.

Recent advancements in machine learning (ML) offer promising alternatives by utilizing data from numerical simulations, low-fidelity models, or measurements. For example, Mungiole and Wilson [9] used artificial neural networks trained with parabolic equation simulations to predict outdoor sound transmission loss, and Hart et al. [10] benchmarked various ML techniques against parabolic simulations for atmospheric turbulence effects on sound propagation. Pettit and Wilson [11] recently employed Physics-Informed Neural Networks (PINNs) trained on parabolic equation simulations to predict outdoor sound propagation. However, direct application of ML methods to approximate the solution to the LEE currently remains unexplored.

This study investigates the effectiveness of Physics-Informed Neural Networks (PINNs) and Fourier Neural Operators (FNOs) in approximating solutions to the LEE for outdoor acoustic propagation. We evaluate how additional training data enhances PINN performance and assess the predictive capability of FNOs trained solely on numerical simulation data.

Methods

Linearized Euler Equations

The Linearized Euler Equations (LEE) describe acoustic wave propagation in a moving atmosphere through perturbations in acoustic velocity $\mathbf{u}_{\text{acc}}$ and pressure p_{acc}:

$$\frac{D\mathbf{u}_{\text{acc}}}{Dt} + (\mathbf{u}_{\text{acc}} \cdot \nabla)\mathbf{u}_{\text{met}} = -\frac{1}{\rho_{\text{met}}}\nabla p_{\text{acc}},$$
$$\frac{Dp_{\text{acc}}}{Dt} + (\mathbf{u}_{\text{acc}} \cdot \nabla)p_{\text{met}} = -\kappa p_{\text{met}}\nabla \cdot \mathbf{u}_{\text{acc}}.$$

Here, $\frac{D}{Dt} = \frac{\partial}{\partial t} + (\mathbf{u}_{\text{met}} \cdot \nabla)$ is the material derivative, $\mathbf{u}_{\text{met}}$ and p_{met} represent the background atmospheric velocity and pressure, ρ_{met} is the atmospheric density, and κ is the adiabatic index [4, 5]. In this formulation, density and thermodynamic property variations due to acoustic perturbations are assumed negligible, simplifying the equations.

Physics-Informed Neural Networks (PINNs)

Physics-Informed Neural Networks (PINNs) incorporate the governing physical laws directly into the learning process by minimizing the residuals of the underlying PDEs during training [12]. The total loss function is composed of multiple components:

$$\mathcal{L}_{\text{PINN}} = \underbrace{\|\text{Res}_u\|^2 + \|\text{Res}_p\|^2}_{\text{PDE residuals}} + \mathcal{L}_{\text{IC}} + \mathcal{L}_{\text{BC}} + \mathcal{L}_{\text{Data}},$$

where the first two terms ensure the neural network predictions satisfy the Linearized Euler Equations. The initial condition loss $\mathcal{L}_{\text{IC}}$ penalizes deviation from known initial states at $t = 0$, while $\mathcal{L}_{\text{BC}}$ enforces consistency at the spatial boundaries. If available, additional measurement or simulation data are incorporated via $\mathcal{L}_{\text{Data}}$.

The PDE residuals are evaluated using automatic differentiation applied to the network output. For the LEE, the residuals for the acoustic velocity $\mathbf{u}_{\text{acc}}$ and acoustic pressure p_{acc} are defined as:

$$\text{Res}_{\mathbf{u}} = \frac{D\mathbf{u}_{\text{acc}}}{Dt} + (\mathbf{u}_{\text{acc}} \cdot \nabla)\mathbf{u}_{\text{met}} + \frac{1}{\rho_{\text{met}}}\nabla p_{\text{acc}},$$
$$\text{Res}_p = \frac{Dp_{\text{acc}}}{Dt} + (\mathbf{u}_{\text{acc}} \cdot \nabla)p_{\text{met}} + \kappa p_{\text{met}}\nabla \cdot \mathbf{u}_{\text{acc}}.$$

The neural network is trained to minimize $\mathcal{L}_{\text{PINN}}$ over a set of collocation points $\{x_i, y_i, t_i\}$ sampled across the spatio-temporal domain. By embedding the structure of the governing equations, PINNs offer an effective framework for solution approximation in physics-based problems where labeled data may be limited or sparse.

Fourier Neural Operators (FNOs)

Fourier Neural Operators (FNOs) are a class of neural networks designed to learn mappings between function spaces, making them well-suited for solving partial

differential equations (PDEs) [13]. Instead of learning pointwise mappings, FNOs learn the global operator that maps an input function to an output function (wind velocity field to acoustic pressure field in our case).

Given an operator $\mathcal{G} : \mathcal{A} \to \mathcal{U}$, where $a(x) \in \mathcal{A}$ and $u(x) \in \mathcal{U}$, FNOs aim to approximate $u(x) = \mathcal{G}(a)(x)$. The update rule for each layer of the FNO is:

$$v_{t+1}(x) = \sigma\left(W v_t(x) + \mathcal{F}^{-1}\left(R \cdot \mathcal{F}(v_t(x))\right)\right),$$

where $v_t(x)$ is the feature representation at layer t, W is a learnable local linear operator (e.g., 1×1 convolution), $\mathcal{F}$ and $\mathcal{F}^{-1}$ denote Fourier and inverse Fourier transforms, R is a learnable weight tensor applied in the frequency domain, and σ is a nonlinear activation function.

By working in the frequency domain, FNOs efficiently capture global patterns and long-range dependencies, which are particularly relevant for modeling wave propagation problems and once trained, FNOs can rapidly infer new solutions for varying input fields. In this study, FNOs are trained using synthetic datasets generated from high-fidelity finite-difference solver of the Linearized Euler Equations (LEE).

Results and Discussion

Impact of Snapshot Data on PINN Accuracy

Table 1 summarizes the simulation and network parameters used in this study. We compare the effect of snapshot data on PINN accuracy by training two networks: one with only initial and boundary conditions, and another with additional snapshot data.

Table 1: Parameter settings for snapshot data impact study.

Parameter	Value
Domain	$x, y \in [-100, 100]$ m
Simulation Time	$t \in [0, 1]$ s
Flow Velocity	5 m/s (x-direction)
Initial Condition	Gaussian pressure, $\sigma = 5$ m
Collocation Points	50,000 random points
IC Points	5,000 points at $t = 0$ s
BC Points	3,000 points (750 per side)
Snapshot Points	2,000 points at $t = \{0.2, 0.4, 0.6, 0.8\}$ s
Architecture	6 hidden layers, 80 neurons each
Activation	SIREN ($\omega_0 = 1$)
Optimizer	Adam (lr=10^{-3}, decay=10^{-4})

Figure 1 presents snapshots of acoustic wave propagation at selected simulation times, comparing results from the Finite Difference (FD) method (ground truth), Physics-Informed Neural Network trained only on initial and boundary conditions (PINN IC+BC only), and PINN additionally trained with snapshot data (PINN IC+BC+Snapshots).

The inclusion of finite-difference snapshot data improves the accuracy of the PINN predictions at later simulation stages. Table 2 quantifies the performance of both PINN approaches compared to the ground truth. At t=0.2 s, the standard PINN performs slightly better in terms of L2 relative error because, at this early stage, the wave behavior is predominantly governed by the initial conditions. The additional snapshot data introduces an extra loss term that, without a dedicated training strategy (such as [14]), can slightly compromise early-time convergence. However, at t=0.6 s, the snapshot-enhanced PINN shows clear advantages across all error metrics, emphasizing the effectiveness of incorporating additional data to capture the complex wave interactions that develop over time.

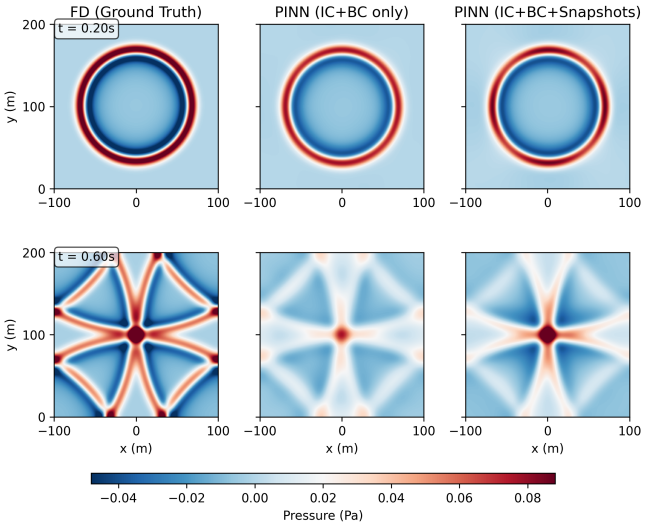

Figure 1: Snapshots of acoustic wave propagation comparing FD (ground truth), PINN (IC+BC only), and PINN with additional snapshot data.

Table 2: Error metrics comparison between PINN (IC+BC) and PINN+ (IC+BC+Snapshots) at two times.

	t=0.2 s		t=0.6 s	
Metric	PINN	PINN+	PINN	PINN+
L2 Rel. Error (%)	30.19	33.37	69.64	60.06
Max Rel. Error (%)	37.28	44.42	61.93	52.03
Mean Abs. Error	0.0047	0.0055	0.0176	0.0146

In this study, the additional data used were full-field pressure snapshots at specific timesteps obtained from a high-fidelity simulation. These snapshots serve as spatially dense supervision signals, complementing the sparse initial and boundary data. This is different from typical measurement data, which often consists of time series at fixed sensor locations but both data can still be used in training PINNs to better train helping maintain physical consistency across the domain.

Capturing High-Frequency Term using SIREN

In our problem of modeling outdoor acoustic waves using LEE, accurately capturing high-frequency components is crucial, especially when dealing with an oscillatory source term. SIREN (Sinusoidal Representation Networks) [15] use a sine-based activation function given by

$$\sigma(z) = \sin(\omega_0\, z), \tag{1}$$

where ω_0 is a tunable parameter that scales the activation frequency. This activation function is particularly effective for our task, as it naturally represents the oscillatory behavior present in acoustic wave propagation.

Table 3: Parameter settings for high-frequency source term study using SIREN.

Parameter	Value
Domain (1D)	$x \in [0, 200]$ m
Simulation Time	$t \in [0, 1]$ s
Mean Flow Velocity	∼0.001 m/s
Initial Pressure	Gaussian source (σ=2 m), amplitude=1.0, frequency=5 Hz
Collocation Points	20,000 random points
IC Points	Points sampled at t=0 with p=v=0
BC Points	200 points (100 each at x=0 and x=200 m)
Hidden Layers	3 hidden layers with 40 neurons each
Activation Function	SIREN sine activation

Our model now applied a source term with sinusoidal time variation at a frequency parameter of $freq = 5.0$ Hz, generating complex wave patterns in the middle. Table 3 presents the simulation and network parameters for evaluating SIREN activation functions with high-frequency source terms.

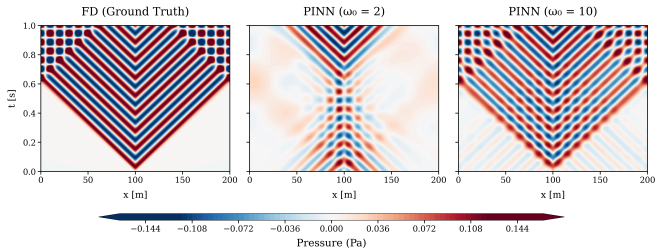

Figure 2: Impact of different ω_0 values on the representation of high-frequency components in the acoustic field. Higher ω_0 values capture finer details but require careful tuning for stability.

Table 4 quantifies the performance differences between PINN models using different ω_0 values against the finite difference ground truth. The PINN with $\omega_0 = 10$ shows substantial improvements across all error metrics compared to $\omega_0 = 2$, with a 59% reduction in L2 relative error and 58% lower mean absolute error.

Table 4: Error metrics comparison between PINN models with different SIREN frequency parameters (ω_0).

Metric	$\omega_0 = 2$	$\omega_0 = 10$
L2 Rel. Error (%)	90.18	37.05
Max Norm. Error (%)	53.26	28.82
Mean Abs. Error	0.0490	0.0207

Physically, the improvement with higher ω_0 values can be understood through the network's enhanced ability to represent the spatial variations created by our source. The higher $\omega_0 = 10$ configuration allows the neural network to more effectively capture the steep gradients near the Gaussian source and the resulting higher frequency wave patterns throughout the domain.

With $\omega_0 = 2$, the pressure field exhibits noticeable phase errors and amplitude attenuation. In contrast, $\omega_0 = 10$ maintains proper wave characteristics across the domain, correctly modeling the physics of the LEE system with our specified source parameters.

Our experiments demonstrate that tuning ω_0 appropriately captures the necessary high-frequency details while maintaining stable training without adding network complexity. This targeted use of SIREN activations proves essential for achieving accurate acoustic simulations in our LEE framework.

Fourier Neural Operator (FNO) Predictions under Varying Wind Conditions

Figure 3 presents the results of the Fourier Neural Operator (FNO) model, which predicts sound pressure fields from input wind velocity fields. The training and evaluation data were generated using AKU3D, a FDTD LEE solver [7]. Table 5 summarizes the simulation parameters along with the FNO architecture and training settings used in this study. The input comprises a two-dimensional wind velocity field (wind speed in the x-direction) with a sinusoidal acoustic source centrally located. Two representative wind profiles are examined: one with a lower velocity gradient and another with a higher velocity gradient.

Table 5: Parameter settings for FNO model under varying wind conditions.

Simulation Parameters	
Domain	$x, y \in [0, 100]$ m
Source Loc.	(100, 50) m
Freq.	5 Hz
Wind Profiles	Logarithmic gradient (low and high)
FNO Architecture and Training Settings	
FNO Layers	4
Fourier Modes	12
Padding	9
Training Steps	10,000
Batch Size	32

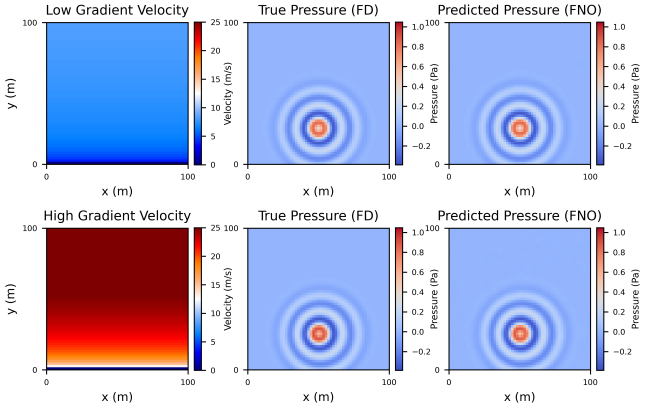

Figure 3: FNO predictions for two wind profiles: (left to right) input wind field, AKU3D-simulated pressure field, FNO-predicted pressure field, and corresponding pressure difference.

Table 6 quantifies the prediction accuracy for both wind profiles. The FNO performs best in scenarios with gentle wind gradients, showing minimal deviation from the reference simulation. As the wind gradient steepens, the prediction error increases only slightly but remains within a similar range, highlighting the model's resilience

to moderate increases in atmospheric complexity.

Table 6: Error metrics for FNO predictions under different wind velocity gradients.

Metric	Low Gradient	High Gradient
L2 Rel. Error (%)	1.15	3.30
Max Rel. Error (%)	0.98	3.47
Mean Abs. Error	0.00093	0.00247

Summary and Outlook

This study explored the potential of Physics-Informed Neural Networks (PINNs) and Fourier Neural Operators (FNOs) to approximate solutions to the Linearized Euler Equations (LEE) for modeling outdoor acoustic wave propagation, demonstrating that both methods can leverage data compared to traditional numerical solvers.

PINNs ensure physical consistency by incorporating the governing PDEs along with initial and boundary conditions. Adding data can further improve accuracy at later timesteps, though it also introduces additional complexity during training, as the model must balance multiple loss components. Nevertheless, PINNs remain a versatile tool that can combine physics-based constraints with available data to capture wave dynamics.

FNOs demonstrated predictive performance by learning directly from high-fidelity simulation data. They accurately modeled acoustic wave propagation under varied atmospheric conditions, with only a slight decrease in accuracy under increasingly complex wind profiles. Future improvements for FNOs might involve incorporating more complex atmospheric input data instead of relying solely on simple 2D scalar fields.

Looking ahead, future research should explore alternative methods to overcome convergence challenges common in iteratively optimized PINN approaches. In addition, testing the robustness of FNO models under more complex atmospheric conditions and input structures, extending these models to three-dimensional simulations, and validating predictions against experimental measurements are critical directions for advancing practical applications. The insights gained from these efforts could ultimately facilitate the development of accurate, ML-based surrogate models for rapid acoustic predictions.

References

[1] Maarten Hornikx. Ten questions concerning computational urban acoustics. *Building and Environment*, 106:409, 2016. doi: 10.1016/j.buildenv.2016.06.028.

[2] J. E. Piercy, T. F. W. Embleton, and L. C. Sutherland. Review of noise propagation in the atmosphere. *Journal of the Acoustical Society of America*, 61(6):1403–1418, 1977. doi: 10.1121/1.381455.

[3] Rohan Kapoor, Niels Kloet, Alessandro Gardi, Assem Mohamed, and Roberto Sabatini. Sound propagation modelling for manned and unmanned aircraft noise assessment and mitigation: A review. *Atmosphere*, 12(11):1424, 2021. doi: 10.3390/atmos12111424.

[4] Chun–Wei Tam. Computational aeroacoustics: Issues and methods. *AIAA Journal*, 33(10):1788–1796, 1995. doi: 10.2514/3.12828.

[5] Christophe Bailly and Daniel Juve. Numerical solution of acoustic propagation problems using linearized euler equations. *AIAA Journal*, 38(1):22–29, 2000. doi: 10.2514/2.949.

[6] Dick Botteldooren. Finite-difference time-domain simulation of low-frequency room acoustic problems. *Journal of the Acoustical Society of America*, 98(6):3302–3308, 1995. doi: 10.1121/1.413830.

[7] Reinhard Blumrich and Dietrich Heimann. A linearized eulerian sound propagation model for studies of complex meteorological effects. *The Journal of the Acoustical Society of America*, 112(2):446–455, 2002.

[8] Nicolas Morales, Vivek Chavda, Ravish Mehra, and Dinesh Manocha. MPARD: A high-frequency wave-based acoustic solver for very large compute clusters. *Applied Acoustics*, 121:82–94, 2017. doi: 10.1016/j.apacoust.2017.01.009.

[9] Michael Mungiole and D. Keith Wilson. Prediction of outdoor sound transmission loss with an artificial neural network. *Applied Acoustics*, 67(4):324–345, 2006. doi: 10.1016/j.apacoust.2005.06.003.

[10] Carl R. Hart, D. Keith Wilson, Chris L. Pettit, and Edward T. Nykaza. Machine-learning of long-range sound propagation through simulated atmospheric turbulence. *The Journal of the Acoustical Society of America*, 149(6):4384–4395, 2021. doi: 10.1121/10.0005280.

[11] Chris L. Pettit and D. Keith Wilson. A physics-informed neural network for sound propagation in the atmospheric boundary layer. *Proceedings of Meetings on Acoustics*, 42(1):022002, 2021. doi: 10.1121/2.0001383.

[12] Maziar Raissi, Paris Perdikaris, and George Em Karniadakis. Physics-informed neural networks: A deep learning framework for solving forward and inverse problems involving nonlinear partial differential equations. *Journal of Computational Physics*, 378:686–707, 2019. doi: 10.1016/j.jcp.2018.10.045.

[13] Zongyi Li, Nikola B. Kovachki, Kamyar Azizzadenesheli, Burigede Liu, Kaushik Bhattacharya, Andrew M. Stuart, and Anima Anandkumar. Fourier neural operator for parametric partial differential equations. In *Advances in Neural Information Processing Systems (NeurIPS)*, volume 33, pages 9472–9483, 2020.

[14] Rafael Bischof and Michael A Kraus. Multi-objective loss balancing for physics-informed deep learning. *Computer Methods in Applied Mechanics and Engineering*, 439:117914, 2025.

[15] Vincent Sitzmann, Julien Martel, Alexander Bergman, David Lindell, and Gordon Wetzstein. Implicit neural representations with periodic activation functions. *Advances in neural information processing systems*, 33:7462–7473, 2020.